Precipitation over urban areas in the western Maritime Continent using a convection-permitting model

Daniel Argüeso [1,2,*]

Phone (+61) 2 9385 8488
Email d.argueso@unsw.edu.au

Alejandro Di Luca [2]

Jason P. Evans [1,2]

[1] ARC Centre of Excellence for Climate System Science, University of New South Wales, Sydney, Australia

[2] Climate Change Research Centre, Level 4, Matthews Building, University of New South Wales, Sydney, NSW, 2052 Australia

Abstract

This study investigates the effects of urban areas on precipitation in the western Maritime Continent using a convection-permitting regional atmospheric model. The ₩Weather ₹Research and ₹Forecasting model was used to simulate the atmosphere at a range of spatial resolutions using a multiple nesting approach. Two experiments (with and without urban areas) were completed over a 5-year period (2008–2012) each to estimate the contribution of cities to changes in local circulation. At first, the model is evaluated against two satellite-derived precipitation products and the benefit of using a very high-resolution model (2-km grid spacing) over a region where rainfall is dominated by convective processes is demonstrated, particularly in terms of its diurnal cycle phase and amplitude. The influence of cities on precipitation characteristics is quantified for two major urban nuclei in the region (Jakarta and Kuala Lumpur) and results indicate that their presence locally enhances precipitation by over 30 %. This increase is mainly due to an intensification of the diurnal cycle. We analyse the impact on temperature, humidity and wind to put forward physical mechanisms

that explain such changes. Cities increase near surface temperature, generating instability. They also make land-sea temperature contrasts stronger, which enhances sea breeze circulations. Together, they increase near-surface moisture flux convergence and favour convective processes leading to an overall increase of precipitation over urban areas. The diurnal cycle of these effects is reflected in the atmospheric footprint of cities on variables such as humidity and cloud mixing ratio and accompanies changes in precipitation.

Keywords

Regional climate modelling
Precipitation
Maritime Continent
Urban climate
Convection
Convection-permitting models

Electronic supplementary material

The online version of this article (doi:10.1007/s00382-015-2893-6) contains supplementary material, which is available to authorized users.

1. Introduction

World population is becoming increasingly urban and is progressively concentrated in large urban agglomerations. Cities alter the atmospheric conditions creating an environment that is clearly different from the natural landscape. This has several implications for many sectors such as health and energy, especially in large cities. Urban areas usually create warmer and drier conditions near the surface, but also perturb wind regimes, atmospheric stability and precipitation. The latter is of major importance because it may affect urban water resources management but also has repercussions in terms of increased vulnerability to rainfall extremes.

The effect of cities on local precipitation has been studied for a few decades now (Atkinson 1971; Changnon 1968; Han et al. 2014; Shepherd 2005) but remains a topic of active research because the driving mechanisms are not fully quantified and mixed responses have been found in recent observational studies. For example, Mishra et al. (2015) found

that most urban areas did not show significant changes in the frequency of precipitation extremes in the recent past, with 17 % of the studied sites showing significant increases, but also 5 % indicating a significant decrease.

Cities have been found to modify precipitation patterns downwind of the city and a number of mechanisms have been suggested for this response (Ackerman et al. 1978; Shepherd 2005). These include atmospheric destabilisation; increased turbulence and mechanical mixing due to increased roughness; diversion of precipitation systems by physical and thermodynamic processes; and modified microphysical processes via aerosol concentration changes. There is also increasing evidence that large coastal cities can influence weather through complex urban land use and weather/climate interactions (Ganeshan et al. 2013; Kusaka et al. 2014; Shepherd 2005). Shepherd (2005) affirms that sea breeze and urban-induced convection acting together may produce preferred regions for convection development. Also, Shepherd and Burian (2003) showed that cities can modify the diurnal cycle of rainfall.

In line with the discussion above, most studies have focused on mid-latitude cities during warm months, when convection plays a central role in generating precipitation. Precipitation in the mid-latitudes is strongly driven by synoptic-scale systems. In such cases, the potential effect of urban areas on precipitation is limited because horizontal and vertical scales of cities are small compared to large-scale systems producing rainfall. Therefore, in order to remove synoptic forced events, existing research has concentrated mostly on summer events, when processes have scales comparable to the extension of cities.

Unfortunately, very few studies investigated the impact of tropical cities on rainfall processes (Comarazamy et al. 2010; Jauregui and Romales 1996) despite the fact that the convective nature of precipitation in such areas makes it more likely to be altered by surface features at the scale of cities. In particular, no research to the authors' knowledge has been conducted to understand urban-induced changes in precipitation over the Maritime Continent.

The Maritime Continent region hosts a number of already large cities that are projected to significantly grow in the future. Quantifying their interaction with local circulation will improve our understanding of the

processes driving local rainfall and is crucial to estimate population exposure to future changes.

Precipitation in the Maritime Continent is interesting because of the intricate configuration of multiple islands with complex topography and spatially variable sea surface temperatures in a warm and shallow ocean. Understanding the processes that models misrepresent or fail to capture in the Maritime Continent is important to accurately describe the climate of the region but also globally, because what occurs in this area strongly feeds back to the large scales that modulate the global climate (Neale and Slingo 2003). One of the key aspects that models simulate inaccurately is the diurnal cycle, which directly defines the precipitation regimes in the Maritime Continent (Gianotti et al. 2012; Love et al. 2011).

This study addresses urban-induced changes in precipitation and the associated mechanisms using a convection-permitting (2-km spatial resolution) regional climate model to simulate the atmosphere and surface processes over the western Maritime Continent. The area includes two major cities located near the coast—Jakarta, Indonesia; and Kuala Lumpur, Malaysia—as well as other urban nuclei within the domain such as Singapore, Bandung, Bogor and Bandar Lampung ~~within the domain~~. Together, they provide a good overview of the urban effects in the region and make it possible to estimate the impact of city size and location on different variables.

An evaluation of the model is also performed, which sheds light on the usefulness of increasing resolution to better resolve fine-scale processes and to improve the representation of precipitation in climate models.

The paper is organized as follows: Sect. 2 describes the modelling experiment and the observational data used; the first part of Sect. 3 is devoted to evaluation of the model and the second part focuses on the urban effects on precipitation; Sect. 4 contains a discussion of the results and the final conclusions.

2. Model and data

2.1. Model description and experiment design

The atmosphere and its interactions with the earth surface in the western

Maritime Continent are simulated using the ~~w~~Weather ~~r~~Research and ~~f~~Forecasting (WRF) modelling system version 3.6 (Skamarock et al. 2009). The model was initialized and driven at the lateral boundaries by ERA-Interim reanalysis (Dee et al. 2011) to provide the best available approximation to the actual atmospheric large-scale conditions. Figure 1 shows the spatial configuration of the model domains. It consisted of a coarser 50-km domain (WRF50) extending from 81.5°E to 157.2°E and 22.5°S to 8.6°N and comprising 168 by 71 grid points. A second 10-km domain (WRF10) with 260 by 220 grid points was located over the western part of the Maritime Continent. Finally, two finer domains at convection-permitting spatial resolution (2 km) were centred in western Java and the southern Malay Peninsula to investigate the interactions between urban areas (red lines in Fig. 1b, c) and the local circulation, and quantify their effects on local precipitation. The model is run over a 5-year period (2008–2012) to sample a broad range of atmospheric conditions and filter out other occasional forcings that might outweigh urban effects in shorter simulations (Kusaka et al. 2014).

Fig. 1

Model domains and topography. **a** Outer domain spans the entire map and nested domains are delimited by *black rectangles*. **b** Domain 3 centred in West Java and **c** domain 4 centred in Southern Malay Peninsula. *Black thick lines* represent the location of vertical profiles for the analysis and *red contour lines* delimit the urban areas

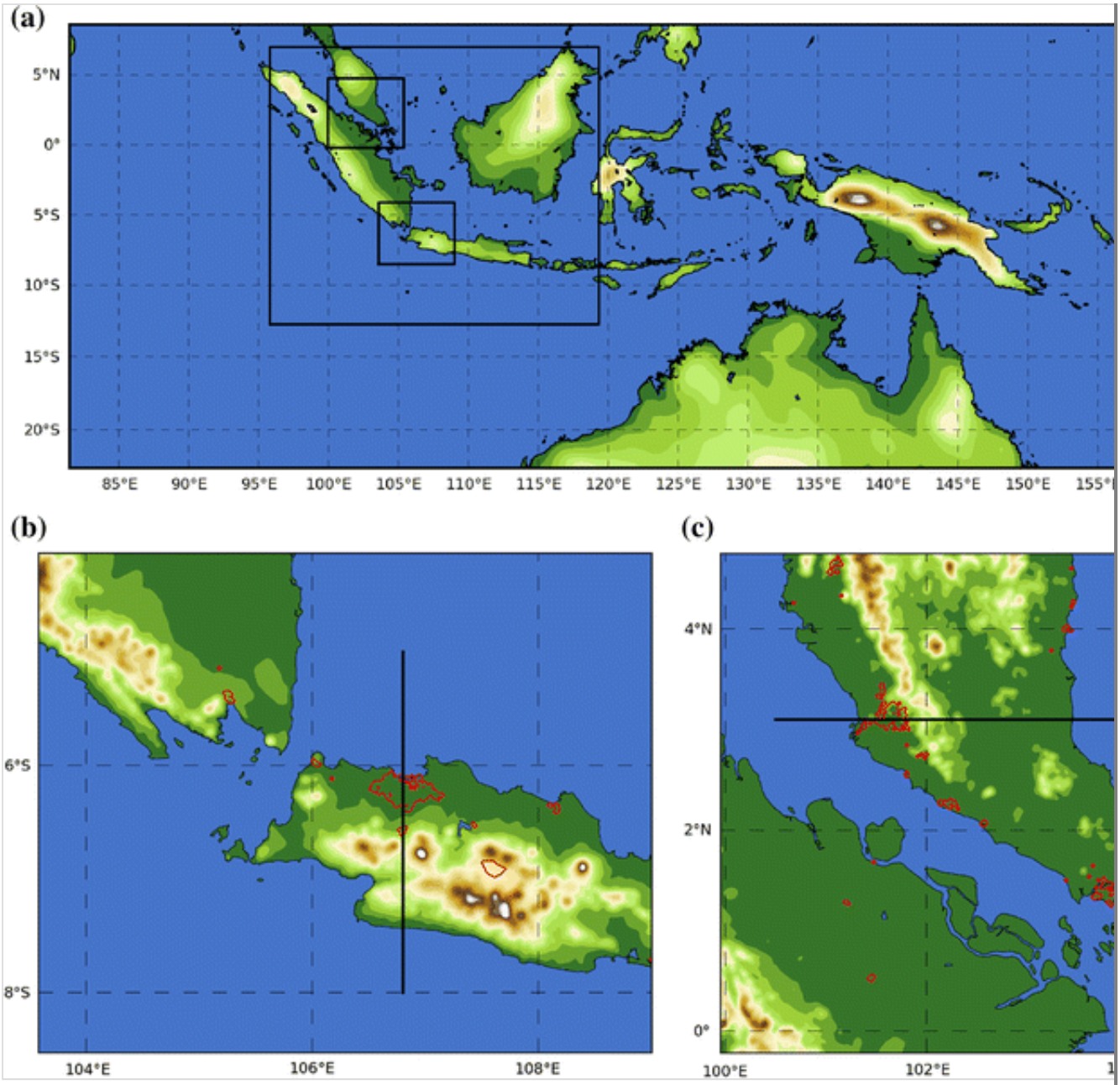

Two experiments were conducted to determine the influence of urban areas on local variables. In both cases the land use information was obtained from MODIS. The difference between them is the inclusion of urban areas and their extension. In the first simulation (WRF2), the original MODIS land use is incorporated into the model as is, while in the second run (WRF2_NoURB), cities were replaced with the dominant surrounding vegetation category (croplands). The role of cities is thus quantified by direct comparison of these two experiments. WRF50 and WRF10 refer to the experiment including cities, which was considered the control run.

Parameterization of sub-grid scale processes included turbulence in the planetary boundary layer (YSU scheme), microphysics (WRF single-moment 6-class scheme), longwave and shortwave radiation (RRTM and Dudhia schemes), and the surface layer (Eta similarity scheme). In

simulations performed using 10- and 50-km grid spacing, the Betts–Miller–Janjic (BMJ) cumulus scheme was chosen to represent sub-grid convective processes. Conversely, in the 2-km grid simulations the cumulus scheme was switched off because convection was assumed to be explicitly resolved. The BMJ scheme used in the outer domains was slightly modified to make it similar to WRF version 2, which was found to give more realistic precipitation climatologies in the tropics (Jullien 2013). In particular, the two efficiency parameters were modified: EFIMN was changed from 0.20 to 0.10 and EFMNT was changed from 0.70 to 0.20. Following Mesinger (2008), the factor to obtain slow profiles over the ocean (FSS) was also changed from 0.85 to 0.825. These schemes were selected based on their simplicity and recommendations from previous studies (Jourdain et al. 2011; Wang et al. 2009).

The land surface processes were simulated with the Noah land surface model. There are two approaches to incorporate urban surfaces into mesoscale models (Kusaka et al. 2001): (1) vary the soil constants (e.g. thermal conductivity and heat capacity) and parameters (e.g., albedo and roughness length) used in the heat balance equation and (2) couple with an urban canopy model. Here the urban environment is represented using the single-layer urban canopy model (SLUCM, Chen et al. 2011; Kusaka et al. 2001), which recognizes the three-dimensional nature of the city as opposed to the default option that simply represent differences in the surface cover. A full description of the parameters used to described the urban areas and the SLUCM coupling with WRF are provided in Chen et al. (2011) and Kusaka et al. (2001). This canopy model was shown to be adequate for spatial resolutions of a few kilometres in contrast with more sophisticated models (Kusaka and Kimura 2004). For simplicity, a single urban density category (high-density residential, default in SLUCM) was assigned to all urban areas.

2.2. Observational data

Satellite-based observational datasets were used to evaluate the model ability to generate realistic precipitation features over western Maritime Continent. The ~~t~~Tropical ~~r~~Rainfall ~~m~~Measuring ~~m~~Mission multi-satellite precipitation analysis 3B42 V7 (hereafter TRMM) on a 0.25° resolution grid and 3-hourly temporal resolution is probably the current reference dataset of its kind for the tropics and therefore was selected in this study.

Details of the algorithm and methodology to create TRMM are provided in Huffman et al. (2007).

In order to better match the model spatial and temporal resolution, and to provide an estimate of discrepancies among satellite-based products, another multi-satellite product generated using the ~~e~~Climate ~~p~~Prediction ~~e~~Center morphing technique (CMORPH, Joyce et al. 2004) at 0.0727° spatial resolution (~8 km near the equator) and 30-min frequency (resampled to hourly frequency here) was used. The resolution of the individual satellite-derived estimates is slightly coarser (~12 by 15 km) and the final resolution was obtained through interpolation. The CMORPH version that blended satellite and rain gauges (CRT) was chosen because the raw version dramatically underestimates precipitation in some areas (Vernimmen et al. 2012) and thus the corrected version is more appropriate for model evaluation purposes.

The adequacy of these datasets (and other high-resolution precipitation grids) to explore tropical precipitation has been previously assessed over different regions (Ebert et al. 2007; Janowiak et al. 2005; Kidd et al. 2010), including the Maritime Continent (Tan et al. 2015; Turk and Xian 2013; Vernimmen et al. 2012). Overall, TRMM was found to provide better estimates of precipitation over western Maritime Continent at monthly scales (Vernimmen et al. 2012), but Ebert et al. (2007) found CMORPH to be superior at daily durations.

Datasets differ considerably near the coast and at high elevations (Vernimmen et al. 2012). Indeed, satellite-derived products are likely to underestimate precipitation in high-elevation areas (Hirpa et al. 2010) and may produce artefacts along the coast due to different retrieval methods over land and ocean. Such differences produce non-negligible uncertainty in the observational datasets that must be considered when evaluating the model performance.

3. Results

3.1. Model evaluation

In this section, we assess the model ability to reproduce characteristics of local precipitation by comparing against two different observation-based datasets. Figure 2 shows the annual precipitation biases over the two

domains of interest centred in western Java and southern Malay Peninsula, hereafter referred to simply as Java and Malay Peninsula. To illustrate the inherent uncertainty of precipitation products derived from satellite observations, annual estimates from both TRMM and CMORPH are shown. Instead of using one of the two datasets as reference to calculate the bias, this uncertainty is also incorporated into its calculation following Evans et al. (2015). If the model estimates are within the range of the observational datasets then we assume them to be equivalent to the observations and we set biases to 0. Otherwise, the bias is estimated with respect to the closest observational value, therefore it is the deviation from the observational range. This comparison quantifies the model performance in terms of total rainfall and how it depends on spatial resolution while taking into account the disparity among observations. All datasets are interpolated using a nearest neighbour approach to match the highest-resolution grid (WRF2 grid) and preserve the original information from each source. It is worth noting that we do not consider uncertainty estimates for individual observation datasets, which would further increase the observational range.

Fig. 2

Annual mean precipitation and model biases in western Java (**a**–**e**) and southern Malay Peninsula (**f**–**j**). Annual mean precipitation from TRMM (**a**, **e**) and CMORPH (**b**, **g**) Annual biases of different model outputs in western Java and southern Malay Peninsula: WRF at 50-km (**c**, **h**), 10-km (**d**, **i**) and 2-km (**e**, **j**) spatial resolution. Biases are calculated with respect to the closest observation-based value and set to zero if model outputs fall within observations. Urban areas are delimited by *green contours*

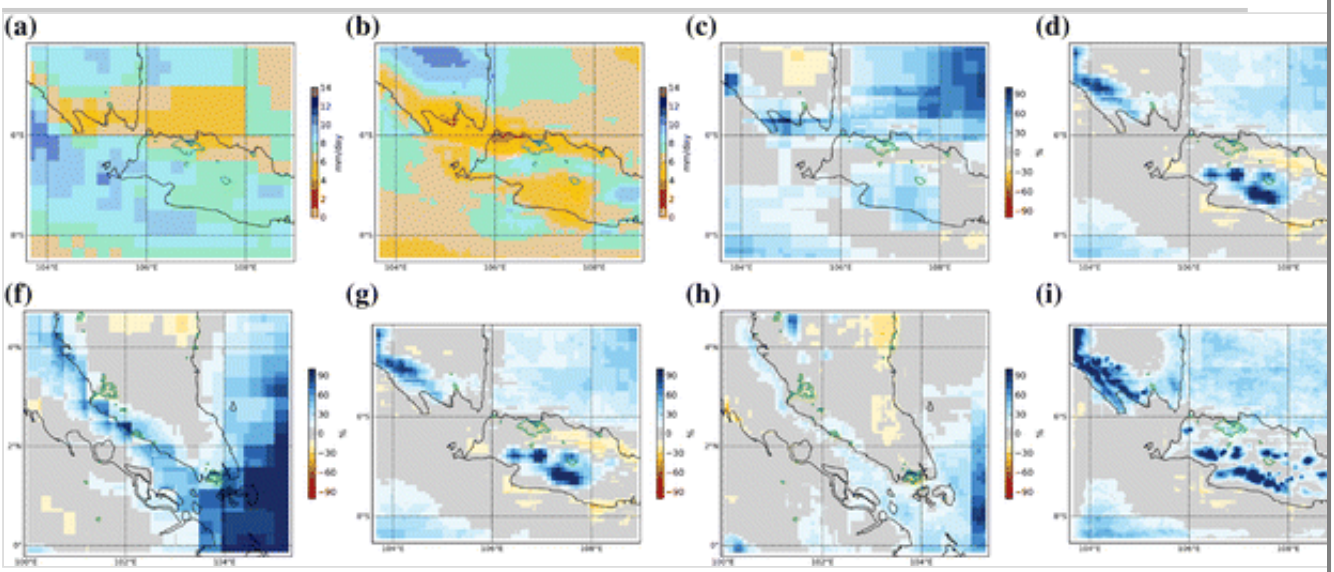

The comparison of CMORPH and TRMM in the Java domain shows that CMORPH tends to produce less precipitation over most of western Java and this part of the Indian Ocean (up to 50 % less in some areas), while it generates more rainfall in the southern part of the Java Sea (30–40 % more), offshore of Jakarta. Differences (WRF minus observations) are generally positive, exceeding 30 % only in inland areas of the Malay Peninsula and the western part of the domain (Strait of Malacca). On the east side of the Malay Peninsula domain, CMOPRH tends to give lower precipitation amounts, being particularly large in the southeast (40–50 % less rainfall).

Overall, WRF tends to generate an excess of rainfall with respect to TRMM and CMORPH, which is in agreement with previous studies also using the Yonsei University scheme (Hong et al. 2006) to parameterise processes in the planetary boundary layer (Ulate et al. 2014). In particular, the model seems to have a tendency towards overestimation over the ocean, which is substantially improved in the 10-km experiments, especially in Malay Peninsula domain. At that resolution, biases with respect to the range of observations are below 10 % in most land areas. The mountainous areas are the exception, but satellite-derived products are known to be troublesome in complex terrain areas (Vernimmen et al. 2012) because they tend to underestimate precipitation in the mountains and typically have coarser spatial resolutions. Therefore differences in such regions should be interpreted carefully. Apart from the high-elevation areas, there seems to be moderate improvement in the Java domain when increasing from 50 to 10 km and a remarkable amelioration in the Malay Peninsula domain. Improvements in total annual estimates are less clear at very high resolution (WRF2). In some instances such as along the coastline in the Malay Peninsula, WRF2 deteriorates WRF10 estimates with respect to satellite-based products, but it should also be remembered that the spatial scale of both TRMM and CMORPH is more comparable to WRF10. In order to take such scale disparity into account, all datasets were rescaled to the coarsest observation dataset (TRMM) using a weighted-area average method. The errors in WRF10 and WRF2 are closer to each other using this approach, but differences still exist that cannot be explained by spatial scales only (Online Resource 1). The magnitude of these deviations is in most cases consistent with or smaller than other previous model evaluations in the region, although their sign might be different (Gianotti et al. 2012; Kwan et al. 2013; Love et al. 2011; Wang et al. 2007).

The patterns of local circulation have a distinct diurnal cycle in the Maritime Continent that translates into a marked diurnal cycle of precipitation, which has traditionally been used as a test for the performance of convective parameterisations (Wang et al. 2007). An aspect that one expects to improve with convection-permitting simulations is the representation of the physical drivers of precipitation and the local circulation that govern convection. A poor simulation of the diurnal cycle and the land-sea breezes in such a complex archipelago has been suggested as a cause of the substantial biases in the Maritime Continent precipitation (Love et al. 2011). Indeed, it is well established that the diurnal cycle of precipitation in the Maritime Continent is one of the key factors that most models struggle to simulate realistically, especially over land (Gianotti et al. 2012; Holloway et al. 2012; Yang and Slingo 2001).

Figure 3 shows the average time of maximum precipitation in a day for different datasets and in local solar time (LST; note that TRMM is only available at 3-hourly frequency). In both domains, there is a clear contrast between land and the surrounding ocean, and even between different ocean areas. This feature is consistent in both satellite products despite their difference in temporal resolution. According to the observation-based datasets, in the Java domain precipitation peaks between 15 and 18H over most of the land, with rainfall maximum occurring slightly earlier in the mountains (12–15H) and later in the day (18–21H) in some coastal regions such as south and east Java and east Sumatra. In the Malay Peninsula, both CMORPH and TRMM indicate that the diurnal precipitation maximum usually occurs at approximately 18H, with the southern tip of the peninsula experiencing an earlier peak (12–15H).

Fig. 3

Time of the precipitation diurnal cycle maximum (in Local Solar Hours) in western Java and southern Malay Peninsula domains from TRMM (**a**, **b**), CMORPH (**b**, **g**), WRF at 50-km (**c**, **h**), 10-km (**d**, **i**) and 2-km (**e**, **j**) spatial resolution. *White grid-boxes* indicate areas where the ratio between the maximum and minimum of the diurnal cycle is <2

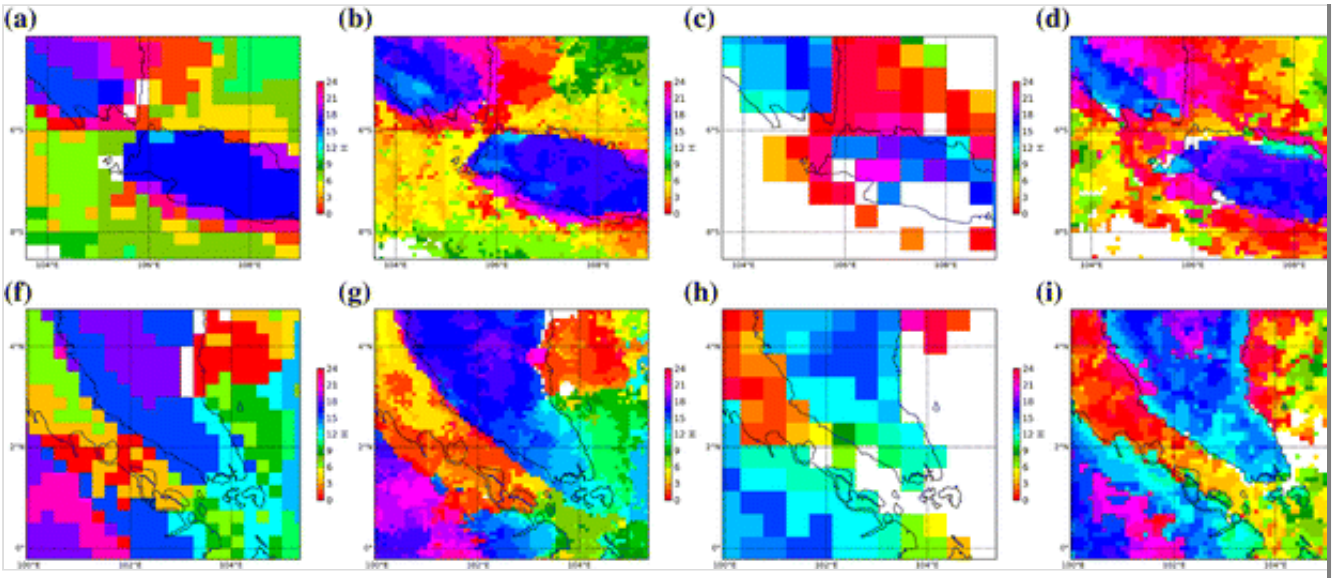

At coarse resolution, WRF begins to hint at such differences (Fig. 3c, h), but islands and topography are too poorly represented to accurately simulate the detailed land-sea contrasts along the coast. The overall pattern is reasonably well simulated, but WRF50 produces precipitation too early compared to observations over land, particularly in the Malay Peninsula (~3 h earlier). It also exacerbates the extension of the coastal transition zone, which extends too far into the ocean and the islands, and the contrast between land and ocean masses is not as marked. Finally, WRF50 does not correctly capture the ocean regime, where the peak is either advanced or delayed depending on the region considered. In fact, WRF50 produces a too weak diurnal cycle over large ocean areas (white areas in Fig. 3) to consider the timing of the maximum to be of any meaning. Coarse-resolution models usually fail to adequately reproduce the observed diurnal cycle and a similar behaviour was also detected in other coarse-resolution models, especially regarding the earlier peak over land (Gianotti et al. 2012; Love et al. 2011).

Higher spatial resolution has a very positive effect in simulating this feature of the diurnal cycle and the model agrees much better with the observations in the timing of the peak. At 10-km resolution, WRF shows higher detail and improves the timing of the maximum in many areas (Fig. 3d, i), although the model still produces the maximum too early, particularly along the coast in the Malay Peninsula domain (3–6 h earlier in the Malay Peninsula and up to 12 h earlier in Sumatra). In Java, WRF10 shows an area of land influence that is too large compared to observations, as evidenced by regions near the islands with peaks occurring at between 21 and 03H (Fig. 3d). The areas where the diurnal cycle is not meaningful

due to its amplitude are substantially reduced at 10-km.

At the finest resolution (Fig. 3e, j), WRF improves the time of the maximum diurnal precipitation virtually everywhere in both domains and shows strikingly good performance when compared to CMORPH, which has higher temporal and spatial resolution than TRMM. It also reduces the areas with no marked diurnal cycle to very isolated grid points. WRF2 simulates the propagation of the diurnal maximum of precipitation from the mountains (~12H) to coastal areas (~21H) in Java and Sumatra. It also shows a similar feature in Malay Peninsula, although it is not present in CMORPH, where precipitation in the interior generally follows that of the coast. This is probably the only exception where the improvement from WRF2 is arguable. Otherwise, the model better captures the timing along the coast, also in the Malay Peninsula domain, with rainfall mostly falling at approximately 15–18H. It is remarkable how the model is able to reproduce the earlier peaks (~12–15H) in the southern tip of the Malay Peninsula and the spatial distribution of the timing of maximum precipitation over Sumatra.

Not only over land does high resolution bring improvements in terms of the diurnal maximum, but also over the ocean. WRF2 better represents the time of maximum rainfall over the Indian Ocean and the Java Sea, where it ranges from 06H in the domain corners to 00H near the land masses, reaching values ~21H in some regions along the coast. Despite the fact that the land influence still extends too far into the ocean, WRF2 shows improvement with respect to WRF10. The influence of the land is limited in high-resolution runs and closer to the observations. Therefore, the maximum of precipitation occurs in the morning in the observations and 2-km WRF in West Java domain, while coarse resolution suggest that the maximum tends to occur during the night. In the Malay Peninsula domain, there is a contrast between the west and the east side of the peninsula, particularly in CMORPH, which is also produced by the high-resolution run. WRF2 also produces spatial patterns that are noisier than observations over the ocean. Love et al. (2011) also found noisier patterns over the ocean, although the scales at which the phases of the diurnal cycle became incoherent were larger than in our experiments, very likely due to differences in the horizontal resolution of the models.

Figure 4 shows the amplitude of the precipitation diurnal cycle for all

datasets calculated as the difference between the diurnal cycle maximum and minimum. Both observational datasets show a clear pattern dominated by the land–ocean contrast in the amplitude of the diurnal cycle, especially in the Java domain. In the Malay Peninsula domain, there is an interesting feature over the Strait of Malacca, where precipitation shows a strong diurnal cycle. On the whole, both TRMM and CMORPH agree in the way they represent the amplitude of the diurnal cycle, although CMORPH tend to provide larger values and finer detail over land.

Fig. 4

Amplitude of the precipitation diurnal cycle in western Java and southern Malay Peninsula domains from TRMM (**a**, **b**), CMORPH (**b**, **g**), WRF at 50-km (**c**, **h**), 10-km (**d**, **i**) and 2-km (**e**, **j**) spatial resolution

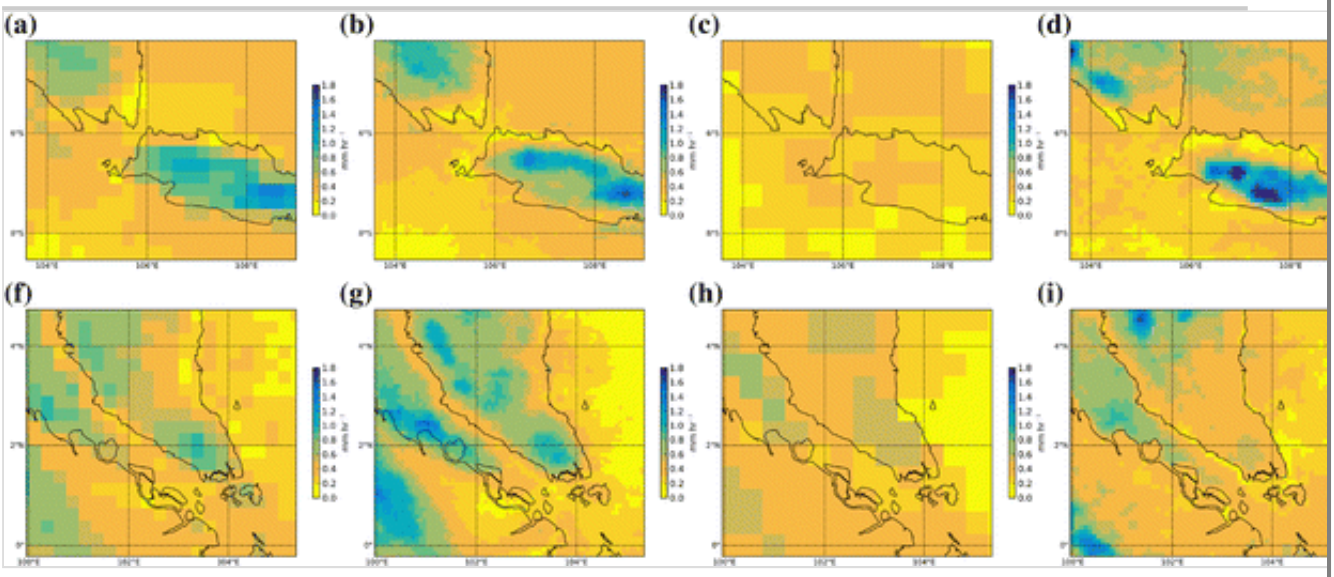

The benefit of increasing resolution from 50 to 10-km is even clearer here than in the timing of the maximum (Fig. 3). At 50-km, WRF is unable to differentiate between land and ocean in terms of the diurnal cycle amplitude over Java and it only hints at some contrast in the Malay Peninsula domain. It does capture the maximum in the Strait of Malacca. At 10-km, the richness of detail is much higher and the model is able to represent the stronger diurnal cycle that characterises the mountainous areas (>1.4 mm hr^{-1}), as well as the coastal transition (0.0–0.2 mm hr^{-1}). Increasing resolution up to 2-km mainly enhances the amplitude of the diurnal cycle and it adds further detail due to better representation of the coastlines and topography. For example, it is noteworthy that the model is able to differentiate the regimes in the Riau Archipelago (south of the Malay Peninsula), which is suggested in TRMM, but missing in all other

datasets except WRF2. The intensification of the precipitation diurnal cycle amplitude leads to better agreement with observations in some cases (Strait of Malacca, South of Malay Peninsula), but generally introduces overestimation. However, it should be remembered that spatial scales in CMORPH and TRMM are more comparable to WRF10 than WRF2 scales.

Further detail in how the model captures the diurnal cycle over two major urban areas (Jakarta and Kuala Lumpur) is provided in Fig. 5, which compares all datasets including the simulation without urban areas. This is for two particular locations near the coast, where the diurnal cycle is especially difficult to simulate because they are at the boundary between inland and offshore precipitation regimes. All datasets are interpolated to the finest grid using a nearest neighbour approach and only urban grid points are considered. Therefore, the results are an area-weighted average of all grid points overlapping with urban areas as defined in the 2-km grid (Fig. 5c, d).

Fig. 5

Diurnal cycle of precipitation over Jakarta (**a**) and Kuala Lumpur (**b**) urban grid points for the different datasets. Urban points are marked with *black* areas in **c** and **d**

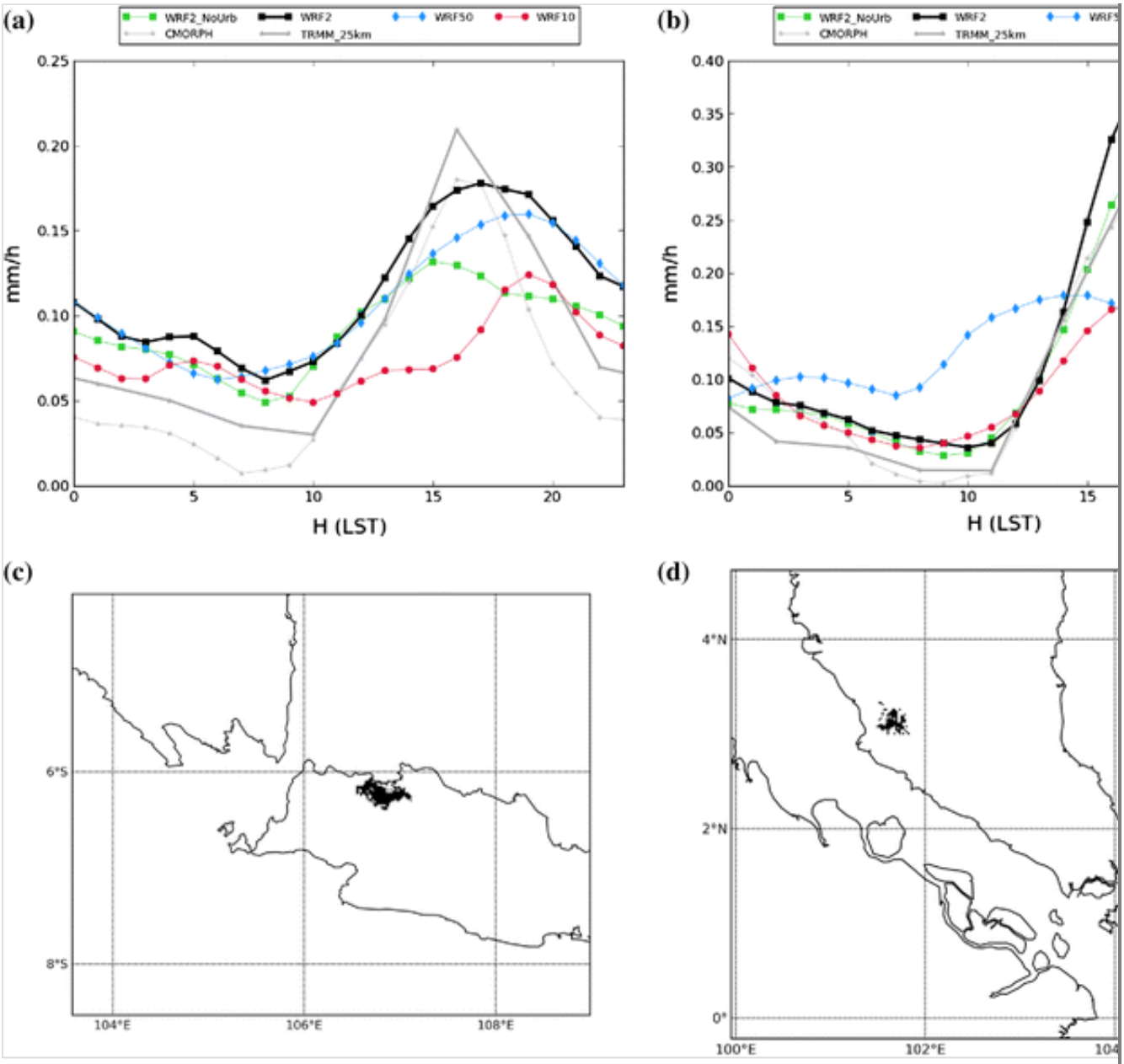

In Jakarta (Fig. 5a), WRF50 and WRF10 produce the peak too late (~19H) in the evening compared to both observations (~16H), while in Kuala Lumpur (Fig. 5b), WRF50 tends to produce the maximum too early (~14H) compared to observations (~17–18H). In both cities the amplitude of the cycle is underestimated in the two coarser simulations (~60 and 50 % underestimation in Jakarta and Kuala Lumpur, respectively). On the other hand, the convection-permitting runs (WRF2 and WRF2_NoUrb) capture the timing of the diurnal cycle very accurately in both locations and visibly improve the coarser-resolution runs. The onset of precipitation maximum in the late morning, the maximum at approximately 17–18H and the decline at 21H produced by WRF2 agrees very well with observations (once again it should be noted that TRMM is available only every 3 h). There remain differences in the magnitude of precipitation throughout the day. For instance, WRF2 overestimates precipitation at almost all times in

Kuala Lumpur and underestimates the amplitude of the cycle in Jakarta. Results from the simulation performed without urban areas (WRF2_NoUrb) are also included in Fig. 5 and show a similar shape of the diurnal cycle though with smaller precipitation rates compared to WRF2. Further analysis between these two simulations is provided later on in Sect. 3.2.

The improvement of the diurnal timing of maximum precipitation with increased resolution places confidence in how the model represents the effects of forcings such as land-sea contrasts and topography, two key factors in modulating rainfall over the Maritime Continent. It also constitutes a step forward in simulating precipitation over the region, improving one of its most critical aspects that models traditionally fail to represent (Teo et al. 2011 and references therein).

This model evaluation ~~places confidence in~~supports the The expression "places confidence" was used in the previous paragraph. For style reasons, we consider it better to use a different expression and decided to use "supports". use of simulated precipitation to study processes occurring in the western Maritime Continent. Despite the fact that substantial biases are still generated by the model, especially in high-elevated regions, we have shown that the model is able to accurately produce valuable features that have traditionally been an issue in the Maritime Continent. Identifying a single cause that explains differences with previous studies is certainly difficult, because the experiments differ in many aspects. However, the benefit of using convection-permitting resolution was established, mostly in terms of the simulation of the diurnal cycle, by comparison with similar coarser resolution simulations. Therefore, the model outputs at higher resolution were deemed more appropriate to investigate rainfall processes, including-urban induced effects. It has also been shown, in agreement with previous research, that notable differences exist between satellite-derived products and therefore, these biases might be partially attributed to uncertainties in the observations and scale disparities between model and observations.

3.2. Urban effects

The influence of cities on the local atmosphere is well known to manifest in multiple ways such as increasing temperature and decreasing humidity (Argüeso et al. 2015; Oke et al. 2006). Figure 6a, b show the temperature

increase induced by urban areas in the model. WRF2 simulates higher mean temperatures when cities are included with values ranging between 1.0 and 1.5 °C in Jakarta, and 1.25 and 2.0 °C in Kuala Lumpur. These increments tend to be larger in the inner parts of the city. Cities also induce a deficit in humidity and the two experiments (Fig. 6c, d, respectively) differ by 0.6–1.2 g kg^{-1} in Jakarta and 1.0–1.4 g kg^{-1} in Kuala Lumpur, which constitutes ~5 and ~8 % of the respective climatological specific humidity when no urban areas are included. The effect is not limited to relatively large cities, but it is apparent in all urban agglomerations regardless of their extension. All urban areas within the domain show to some extent a warmer and drier atmosphere, although city size seems to affect the magnitude of the differences with larger cities showing larger increments. It is interesting to note the exact correspondence between urban areas and the statistical significance of the difference, which is almost exclusively located over and around urban centres, confirming the importance of cities in driving these phenomena. Statistical significance was determined using a Wilcoxon signed-ranked test at a 99 % confidence level for all variables.

Fig. 6

Difference between WRF2 and WRF2 NoUrb in 2-m temperature (**a**, **b**), 2-m specific humidity (**c**, **d**), zonal wind (**e**, **f**), meridional wind (**g**, **h**) and vertical wind in the first 5 levels of the model (**i**, **j**) over Java (*left column*) and Malay Peninsula (*right column*). *Stippling* indicates that differences are statistically significant using a Wilcoxon test at a 99 confidence level using daily values. Urban areas in WRF2 are delimited by *green contours*

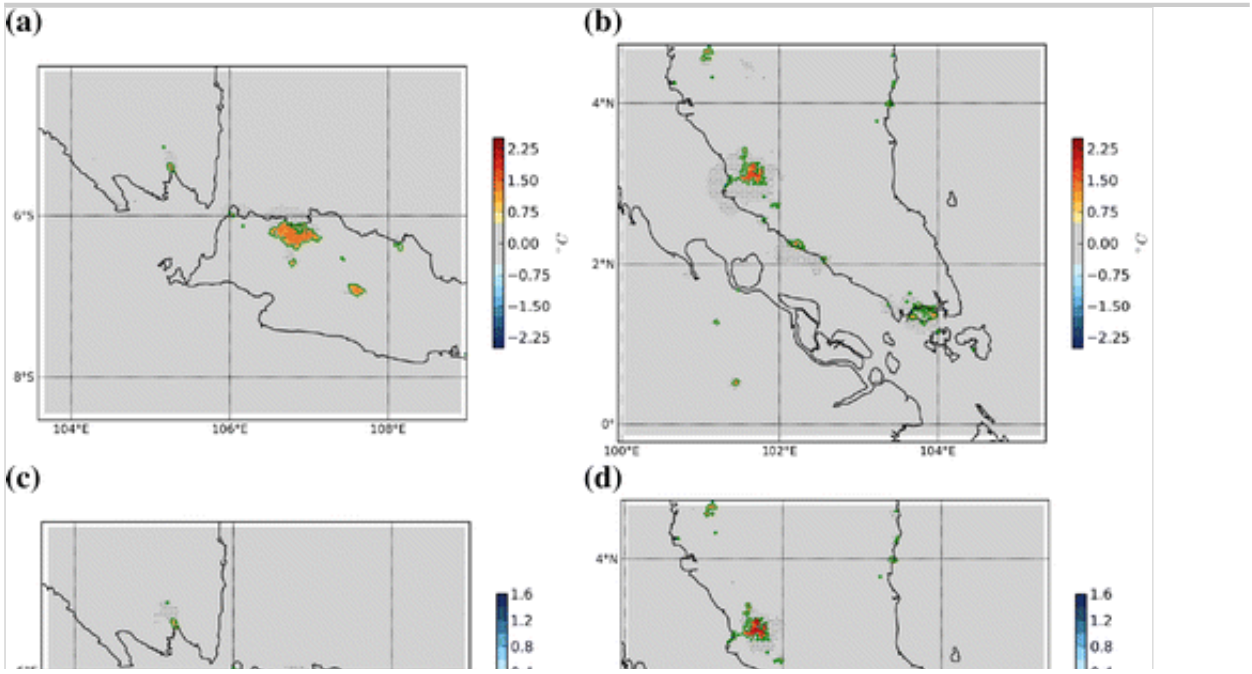

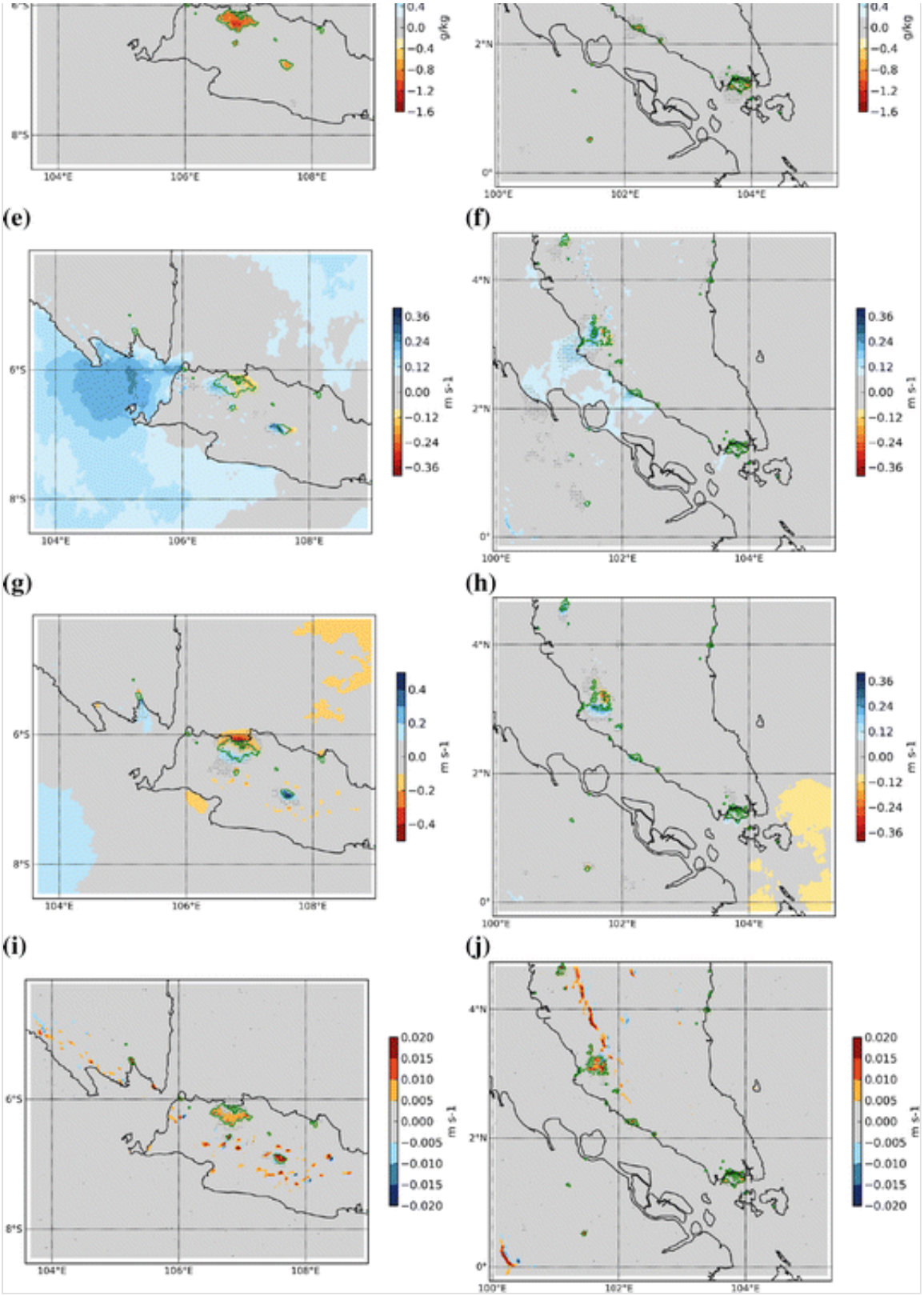

AQ1

It has been found that cities also influence wind due to increased surface drag and increased instability (Childs and Raman 2005). Argüeso et al. (2014) determined that only under light wind regimes (<4 m s^{-1}) did Sydney have a discernible effect on wind speed, though it remained very small. However, in the Maritime Continent sea breeze plays a much more dominant role in defining wind regimes near the coast and so the increased

land-sea contrasts may produce a stronger effect. Figure 6g demonstrates that the presence of Jakarta produces a very local intensification of winds coming from the ocean of up to 0.4 m s^{-1} on average, which constitutes an increase of ~50 % of the mean wind speed in that direction. On the other side of the city, winds are also intensified towards the urban centre and are also statistically significant, but its magnitude is small compared to differences on the coastal side. Winds parallel to the shore (Fig. 6e) also seem to be affected by the presence of Jakarta, but to a lesser extent. Large ocean areas to the west also show differences in winds parallel to the coast of the same magnitude, although these differences are mostly non-significant and thus probably related to the model internal variability. A similar effect is observed in Kuala Lumpur (Fig. 6f, h), where the city strengthens the wind from the ocean, although the importance of sea breeze might be modulated by other factors in this case because it is located further away from the ocean. Also, average simulated wind speeds in the Malay Peninsula are considerably smaller than in Western Java (not shown). It is worth noting that statistically significant differences in wind components are also obtained for smaller cities such as Semarang, Bandung Bandar Lampung and urban centres along the eastern coast of Malay Peninsula.

Figure 6i, j show differences in vertical wind speed integrated over the first five model levels in both domains (approximately the lower 400 m at sea level). Surface warming from urban structures produces instability in the lower atmosphere, as suggested by a lower Convective Inhibition in WRF2 (Online Resource 2). The lifting condensation level and the level of free convection are also higher in WRF2, but PBL is on average deeper over urban areas (120–200 m, not shown) and therefore these levels are more likely reached. Enhanced instability leads to increased vertical speed. In both Jakarta and Kuala Lumpur, vertical wind speed in the first few levels of the model is increased between 0.01 and 0.02 m s^{-1}, which represents a factor 2 increase in Jakarta and factor 3 in Kuala Lumpur with respect to the simulation without cities. Once again, vertical wind speed is consistently increased in all urban areas no matter the extension of the city, although statistical significance is confined to large cities only.

These differences raise the question of whether precipitation is also substantially affected by cities in these two regions. A first glimpse of the differences between the diurnal cycle simulated by WRF2 and

WRF2_NoUrb was provided in Fig. 5. In both Jakarta and Kuala Lumpur, the presence of the city enhances the diurnal maximum of precipitation by over 20 %, but produces little to no changes during the rest of the day.

The comparison of precipitation climatologies from both simulations (Fig. 7) indicates that incorporating cities to the model increases precipitation by more than 30 % over urban areas. In Jakarta, these changes are even larger and reach up to 60 % according to the model. These differences are also detected in Bandung (centre of Java), but are not discernible in smaller urban nuclei, which may imply that a relationship exists between the extension of the city and the effect on precipitation (Shepherd 2005; Schmid and Niyogi 2013). All these changes are statistically significant according to the Wilcoxon test at 99 % confidence level. Despite the fact that significant areas exist beyond urban areas, like for the other variables there is a very good correspondence between urban areas and the significance of precipitation differences.

Fig. 7

Difference between WRF2 and WRF2 NoUrb in total precipitation in Java domain (**a**) and Malay Peninsula domain (**b**). *Stippling* indicates that differences are statistically significant using a Wilcoxon test at a 99 confidence level using daily values. Urban areas in WRF2 are delimited by *green contours*

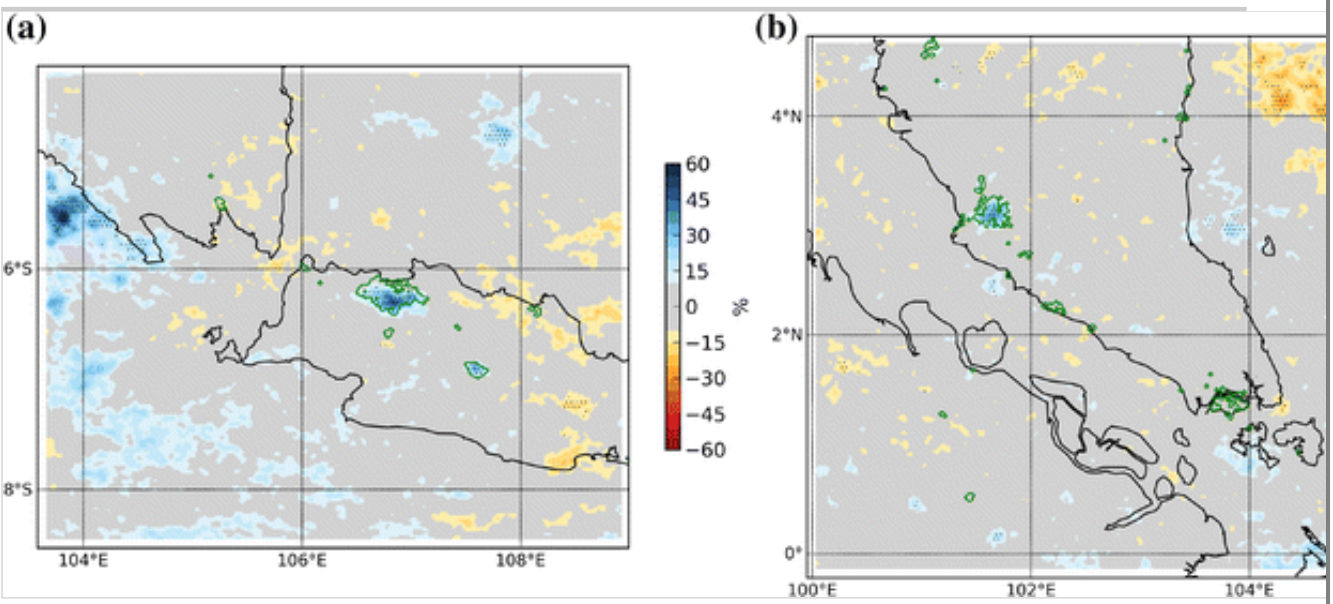

The urban effect on precipitation is usually observed in areas over and downwind of the cities (Han et al. 2014), but in the case of our study, the effect is located over the cities and only in Jakarta it seems to slightly

expand to the south, although differences there are not significant.

In addition to total rainfall, we also analysed changes in the number of rain days (>1 mm day^{-1}) and the mean intensity (total rainfall divided by number of rain days) to ascertain which of the two contributes to larger precipitation amounts over urban areas (not shown). Both precipitation features increase when cities are incorporated in both domains. The number of rain days increases by ~15–20 % in Jakarta and Kuala Lumpur, although in the latter it only increases that much in central areas of the city. Bandung in central Java also undergoes increases in the number of wet days due to the presence of the city. Similarly, the mean intensity of precipitation increases between 15 and 20 % in different parts of Kuala Lumpur and Jakarta, reaching up to 25 and 30 % in the interior, respectively. This suggests that cities in this region impact both frequency and intensity of daily precipitation leading to higher total amounts of rainfall over urban areas.

Figure 8 shows the seasonality of the urban-induced effects (in terms of percentage of total precipitation) along with the monthly precipitation seasonal cycle from WRF2_NoUrb. In Jakarta, precipitation has a strong seasonal cycle dominated by the Southern Hemisphere summer monsoon with the maximum precipitation occurring during the austral summer from December to March (Haylock and McBride 2001). The influence of the city on local precipitation appears to be much stronger, in relative terms, during months when the monsoon is not active (May–Oct) with values attaining 60 % of the WRF2_NoUrb precipitation. This is because during the monsoon months the large-scale circulation associated with the monsoonal winds tends to reduce the local diurnal cycle of land–sea breezes winds (Qian et al. 2010) and it partially outweigh the urban effects. However the effect of the urban areas in precipitation during the wet season is still approximately 10 % according to our experiments. On the other hand, Kuala Lumpur is not strictly affected by the monsoon and has a different seasonal cycle of precipitation, with two maxima, one in April and another in November. In relative terms, the influence of urban-induced effects is fairly similar throughout the year, with a maximum at around March (~40 %) and a minimum in September (~10 %) compared to WRF2_NoUrb. This illustrates that seasonality in the effect of urban areas on precipitation also exist in tropical cities, but it should be noted that it is visible throughout the year. Other large-scale phenomena that could

modulate the sensitivity of precipitation to urban effects such as the Madden–Julian Oscillation or El Niño-Southern Oscillation (Qian et al. 2010) might also make an important contribution, but it remains a topic of future research.

Fig. 8

Seasonal cycle of the difference between WRF2 and WRF2 NoUrb in monthly precipitation (*red*) and monthly precipitation climatology from WRF2 NoUrb (*blue*) using a 3-month running average. Results are shown for Jakarta and Kuala Lumpur urban grid points as shown in Fig. 5c, d

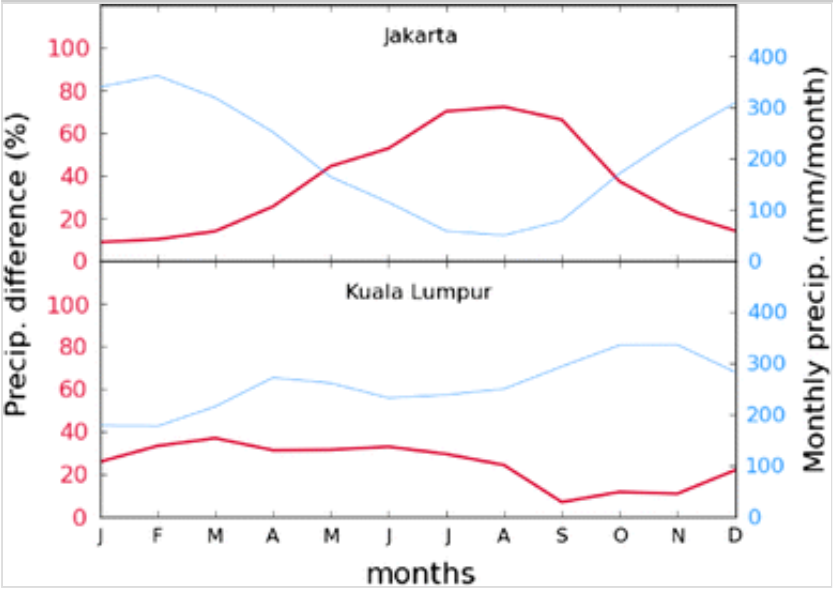

3.2.1. Moisture flux convergence

After the results shown above, we hypothesise that changes induced by the city increase moisture flux convergence near the surface. The vertical displacement of air produced by instability and originated by surface warming has a response in wind convergence in the lower levels. Also, moisture flux convergence has often been linked to convective initiation (Banacos and Schultz 2005) in forecasting applications. Moisture flux convergence was calculated as using the following equation and using the approach described by Bluestein (1992) to deal with discrete variables:

$$MFC = -\nabla \cdot \left(q\mathbf{V}_h\right)$$

where MFC is the moisture flux convergence, q is the water vapour mixing ratio at 2 m and $\boldsymbol{V}_h$ is the horizontal wind vector at 10 m. Figure 9 shows differences in near-surface moisture flux convergence between WRF2 and

WRF2_NoUrb simulations. This comparison indicates statistically significant increases in moisture flux convergence over cities and divergence in the surroundings (negative sign in Fig. 9). Although significant changes are obtained in other locations too, their magnitude is clearly larger in and around urban centres. In areas of Jakarta the differences in convergence reaches up to 9×10^{-4} g kg^{-1} s^{-1}, while the simulation with no cities yields convergence values below 4×10^{-4} g kg^{-1} s^{-1} in most of the area covered by the city except in the centre where it is larger (up to 9×10^{-4} g kg^{-1} s^{-1}). Therefore, moisture flux convergence is at least double when introducing Jakarta. In Kuala Lumpur, differences are even larger (above 9×10^{-4} g kg^{-1} s^{-1} in most of the city) while simulation without cities suggests convergence values below 1×10^{-4} g kg^{-1} s^{-1} and even some areas with average divergence of ~6×10^{-4} g kg^{-1} s^{-1} (not shown).

Fig. 9

Difference between WRF2 and WRF2 NoUrb in moisture flux convergence in Java domain (**a**) and Malay Peninsula domain (**b**). *Stippling* indicates that differences are statistically significant using a Wilcoxon test at a 99 confidence level using daily values. Urban areas in WRF2 are delimited by *green contours*

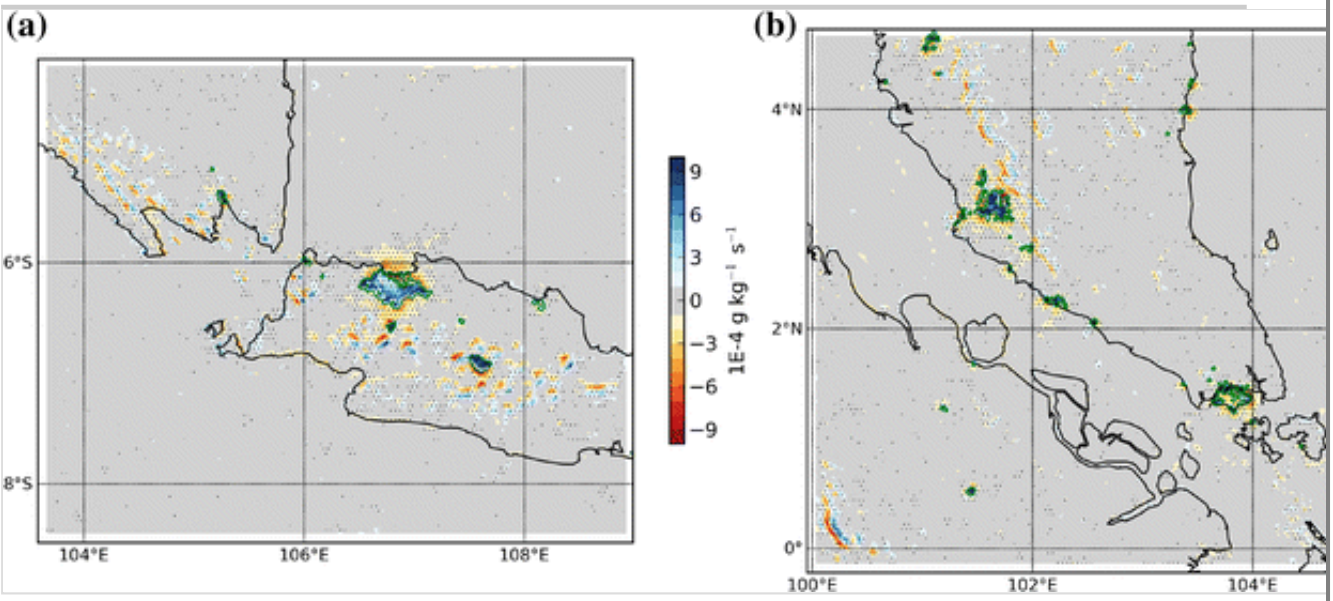

The seasonality of changes in low-level moisture convergence was also analysed (Online Resource 3), but it was found to be approximately the same throughout the year. Therefore, the underlying processes triggered by the city are still present during the wet season, but the large-scale systems outweigh their contribution to precipitation rates during those months.

3.2.2. Vertical profiles of temperature and humidity

The presence of the city enhances near-surface convergence for both moisture and mass in general (not shown), which necessarily perturbs the vertical structure of the atmosphere via destabilization in the lower levels. Anomalies produced at the surface, such as those of temperature and humidity might thus propagate upwards. Figures 10 and 11 illustrate the diurnal evolution of vertical differences in temperature, mixing ratio and cloud mixing ratio between WRF2 and WRF2_NoURB simulations accompanied by differences in the wind components along the vertical plane. As such, they provide information on how far in the vertical the perturbations extend and how they evolve throughout the day. Vertical profiles are located over Jakarta and Kuala Lumpur as indicated by solid red lines in Fig. 1b, c. For the sake of conciseness, only four diurnal snapshots are shown: at 00, 06, 12 and 18H UTC, which correspond to 07, 13, 19 and 01H LST for Jakarta and 06, 12, 18, 00 H LST for Kuala Lumpur.

Fig. 10

Vertical profiles of differences over Jakarta between WRF2 and WRF2 NoUrb in temperature (**a**–**d**), mixing ratio (**e**–**h**) and cloud mixing ratio (**i**–**l**). *Vectors* indicate differences in winds along the vertical plane (note difference in scale between *horizontal* and *vertical winds*). At the *bottom*, ocean is represented in *blue*, urban in *grey* and the rest of land areas in *green*

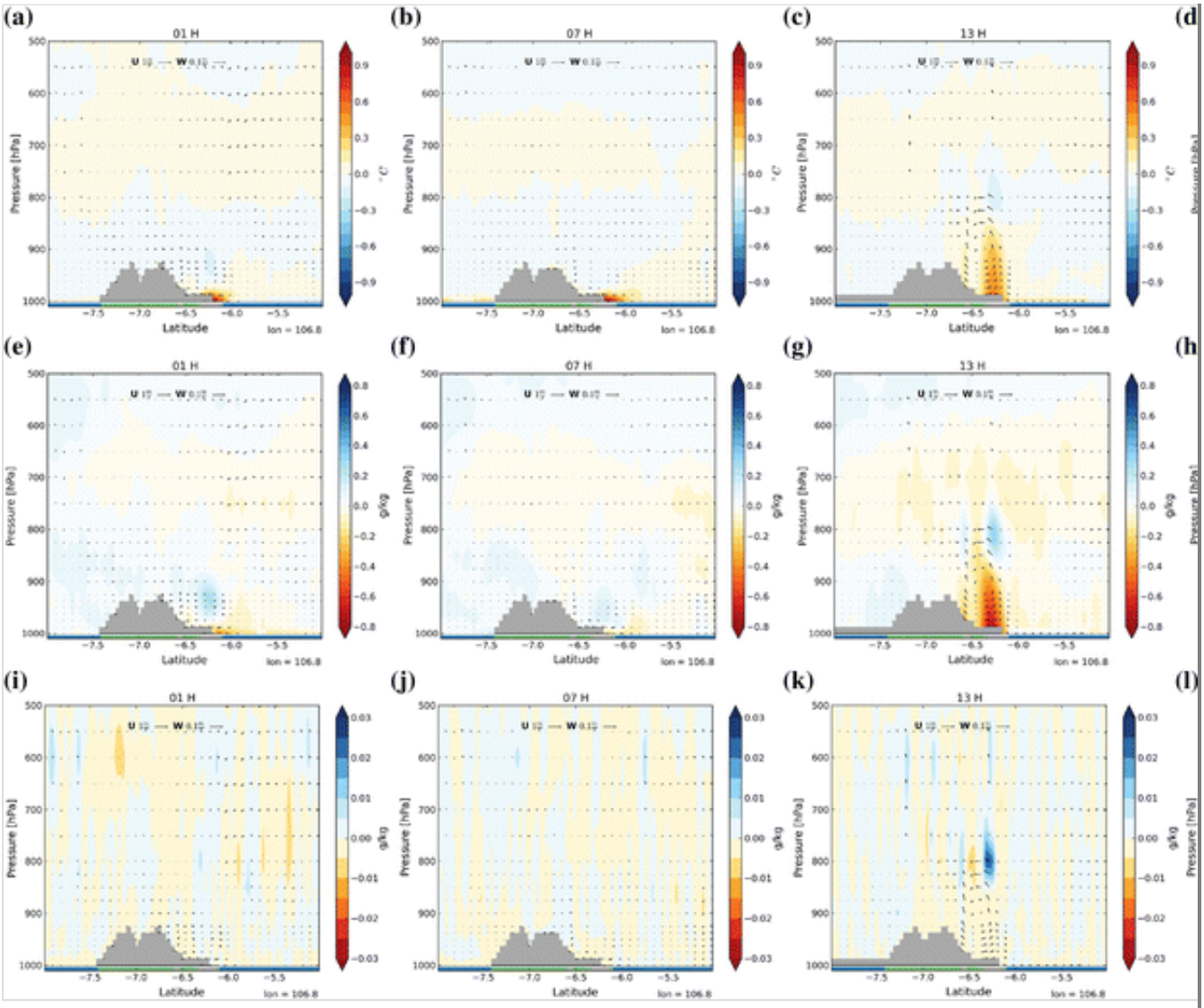

Fig. 11

As Fig. 10 but over Kuala Lumpur

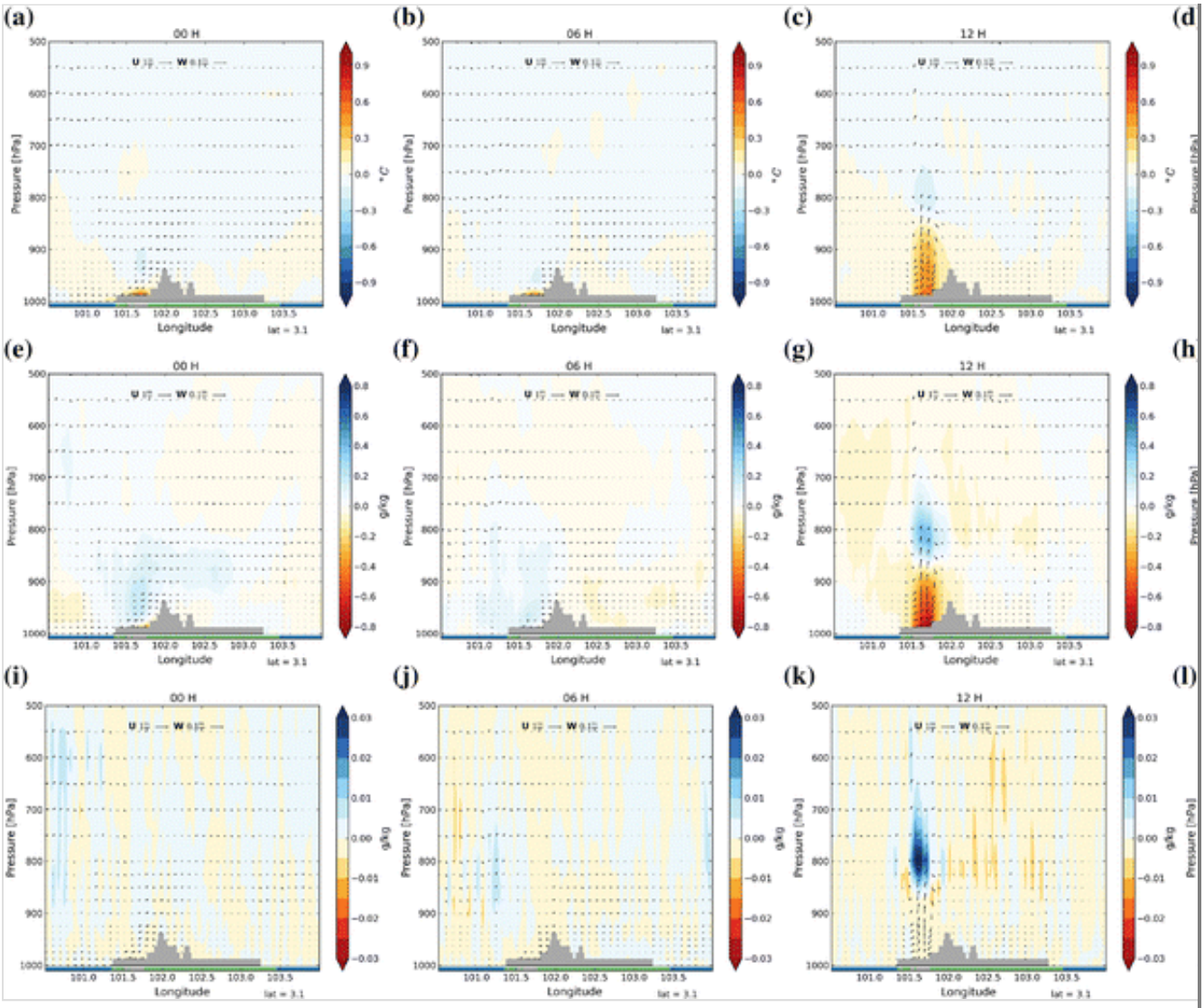

Qualitatively, the response of the atmosphere to urban areas above Jakarta and Kuala Lumpur is very similar, although there are some quantitative differences. The effect of cities on temperature is larger during the night and early morning (Figs. 10a, b, 11a, b) and exceeds 1 °C. However, the difference is limited to the lowest levels (below 975 hPa on average), which is consistent with a stable nocturnal boundary layer. As the day advances, and turbulence starts mixing the lower atmosphere, differences in temperature extend to higher levels and the warming signature is detectable as high as 850 hPa, although they are more moderate and remain on average below 0.6 °C. Above that level, there seems to be a minor cold signature (e.g. Fig. 11c—Kuala Lumpur). During the evening, the planetary boundary layer thins and the urban signature intensifies again and decreases in height back to levels below 900 hPa.

Despite the fact that the air is warmer and thus could hold more vapour in WRF2 than in the WRF2_NoUrb case, cities introduce a water vapour deficit in the lower atmosphere. Changes in wind along the vertical plane

indicate that during the day there is an enhancement of vertical motion that transports air, and therefore humidity, from the surface levels aloft. We previously noted that surface moisture convergence increases due to the presence of the city, which constitutes a positive contribution to the water budget in the lower levels. However, inhibition of surface evaporation typical of urban areas (Argüeso et al. 2014; Cleugh and Grimmond 2011) and vertical transport counterbalance the moisture convergence increase producing a drying net effect in the lower levels. This is consistent with previous findings in Kusaka et al. (2014), where the water budget over Tokyo is investigated.

The net effect is a negative anomaly in the mixing ratio near the surface that reaches ~5 % in both cities during the central hours of the day (Figs. 10g, 11g). Moisture removed from the surface is brought upwards increasing the mixing ratio in the levels above and creating an urban vertical dipole when comparing with the simulation without cities. It develops in the morning (~9–10H LST) and persists throughout the day (until ~22H LST), but it is particularly marked around noon. At that time, the aforementioned negative differences occur and the positive differences above cities take values as large as ~3 % (0.35 g kg^{-1}) in Jakarta and ~4 % (0.4 g kg^{-1}) in Kuala Lumpur. During the night, the dipole almost disappears and only minor negative anomalies are obtained near the surface over cities and slightly positive differences aloft. This is in agreement with previous studies that found a different response of temperature and humidity in urban areas throughout the day (Argüeso et al. 2015) and also with authors that suggested a possible moisture build-up in the early morning (Fig. 11f) despite the suppression of latent heat at the surface due to higher moisture advection (Kusaka et al. 2014).

The impact of urban areas is also detected in cloud mixing ratio (Figs. 10i–l, 11i–l), which substantially increases over cities because uplifted moisture condensates once it reaches the saturation level. The largest differences in cloud mixing ratio between the two simulations occur at approximately 800 hPa and come about at 13H in Jakarta, where it reaches almost 0.03 g kg^{-1} (~60 % increase at that pressure level) and between 12 and 15H in Kuala Lumpur, where it exceeds 0.03 g kg^{-1} (>100 % increase at that pressure level). Vertical differences in cloud mixing ratio begin to be noticeable in the model at around ~10H LST, peak in the afternoon between 12H and 18H LST and dissipate after ~20H LST.

Such a diurnal evolution of the cloud anomaly precedes differences in precipitation among simulations, which tend to be larger in the late afternoon to early evening (16–20H LST, Fig. 5a, b).

Figures 10 and 11 also include differences in winds along the vertical planes to provide further insight in the changes generated by cities. Wind differences suggest that urban areas intensify convective-type circulations with the influence reaching ~800 hPa during the peak times (~12–13H LST). Winds are predominantly from inland during the night and early morning (Online Resources 4 and 5) because the ocean is generally warmer than the land. Urban areas reduce such land-sea contrast and thus the strength of winds is reduced in the lower levels when considering cities (Figs. 10a, b, 11a, b). As for the afternoon (12–13H) and evening (18–19H), there is on average a robust sea-breeze circulation that is intensified near the edge of the urban area. The presence of the city also displaces the convective cell from the coastline towards the city (Online Reources 4c, g and 5c, g).

4. Discussion and conclusions

A set of simulations at varying resolutions from relatively coarse (50-km) to convection-permitting (2-km) were performed over the western Maritime Continent to investigate how local circulation, urbanisation and precipitation interplay in a region that is especially challenging for models.

This study has provided insight into the usefulness of increasing spatial resolution in regional climate modelling studies over the region. We found that increasing spatial resolution up to convective-permitting scales is beneficial in terms of capturing the diurnal cycle, a feature that has traditionally been poorly represented in models and is regarded as a major source of biases (Love et al. 2011). This is in agreement with previous studies that found added value in representing the timing of the diurnal cycle of summertime convection with high-resolution models (Prein et al. 2015). The potential of very-high resolution models resides in the more detailed and coherent picture of the physical processes they provide (see discussion in Di Luca et al. 2015). These results suggest that increasing spatial resolution has a positive impact on the representation of precipitation variability while the long-term averages are not necessarily improved compared to observations. Actually, the model still produces

errors that should not be neglected, especially in high-elevation areas.

Further model development, especially of parameterizations of physical processes such as boundary layer turbulence, is required to improve overall performance at these resolutions. Nevertheless, we expect a better representation of precipitation features other than long-term totals and suggest that the model evaluation needs to focus on characteristics beyond the reduction of biases as we move to convection-permitting resolutions. Nonetheless, disparity among satellite-derived observations might contribute to these biases that can only be partly attributed to model imperfections.

Two sets of multiple-nest simulations with and without urban areas were completed to determine the effect of cities in local atmospheric variables and precipitation. As such we have contributed to existing understanding of the mechanisms by which cities can alter precipitation by examining the particular case of tropical cities in the Maritime Continent.

We found that tropical urban areas in the western Maritime Continent enhance convective processes through changes in the local circulation. Urban areas constitute a source of heat because urban surfaces modify the surface energy flux partitioning channelling latent heat into sensible heat. At the surface, it destabilises the atmosphere in the vertical, which uplifts air masses. To compensate this extra vertical transport, horizontal convergence near the surface is intensified and air from the surroundings is brought over the city. The region is characterized by recurrent sea breezes that are intensified near the surface and thus bring moisture over the city. Because the city continues to heat the near-surface air, destabilization continues in combination with the sea breeze and moisture is uplifted. As a consequence, the convective cell that produces precipitation over land in the late afternoon due to land-sea contrast in temperature is reinforced and shifted over the city increasing local precipitation. Many elements of this phenomenon occur for most cities in the studied domain, but the vicinity of the ocean and the extension of the urban areas are important factors that condition the magnitude of the effect. Han et al. (2014) also proposed a similar sequence of mechanisms, although without the emphasis on the sea breeze contribution.

Our results have shown that cities in the Maritime Continent, and more broadly in the tropics, could have a remarkable impact on local

precipitation rates (>30 % increase in annual rainfall). This is consistent with previous results (Wang et al. 2014) of the effect of urban expansion in the Pearl River Delta. In the tropics, rainfall has a very strong local nature compared to mid latitudes, where synoptic large-scale systems are the dominant driver of precipitation, especially during the cooler months. It is worth noting that seasonality also exists in the influence of cities on precipitation over the western Maritime Continent because of the influence of the monsoon circulation. However, precipitation is strongly modulated during most of the year by land-sea contrasts, which are in turn altered by the presence of urban areas, and therefore these urban impacts are of particular importance in the region.

It must be mentioned that our experiments did not include changes in aerosols and therefore potential changes in nucleation processes are not considered in this study. Also urban areas are characterized by a single high-density urban category; hence the simulations do not include urban heterogeneity, which could affect the spatial pattern and magnitude of the impacts. Finally, waste heat from human activities such as road traffic or industry (i.e. anthropogenic heat) constitutes an additional source of heat and thus destabilization that was not included in these experiments. All these factors need to be investigated individually and in combination to address their relative contribution, however this remains a topic for future research.

Acknowledgments

This work was made possible by funding from the Australian Research Council (ARC) as part of the Centre of Excellence for Climate System Science (CE110001028), as well as the NSW Office of Environment and Heritage. Jason Evans was supported by the Australian Research Council Future Fellowship FT110100576. This work was supported by an award under the Merit Allocation Scheme on the NCI National Facility at the ANU. We are thankful to the European Centre for Medium-Range Weather Forecasts for providing ERA-Interim data. We also thank Dr. Thomas Chubb from Monash University (Australia) for making the Skew-T code publicly available.

5. Electronic supplementary material

Below is the link to the electronic supplementary material.

Supplementary material 1 (PNG 604 kb)

Supplementary material 2 (PNG 539 kb)

Supplementary material 3 (PNG 238 kb)

Supplementary material 4 (PNG 695 kb)

Supplementary material 5 (PNG 806 kb)

References

Ackerman B, Changnon SA Jr, Dzurisin G et al (1978) Summary of METROMEX, volume 2: causes of precipitation anomalies, pp 1–399

AQ2

Argüeso D, Evans JP, Fita L, Bormann KJ (2014) Temperature response to future urbanization and climate change. Clim Dyn 42:2183–2199. doi:10.1007/s00382-013-1789-6

Argüeso D, Evans JP, Pitman AJ, Di Luca A (2015) Effects of city expansion on heat stress under climate change conditions. PLoS ONE 10:e0117066. doi:10.1371/journal.pone.0117066

Atkinson BW (1971) The effect of an urban area on the precipitation from a moving thunderstorm. J Appl Meteorol 10:47–55

Banacos PC, Schultz DM (2005) The use of moisture flux convergence in forecasting convective initiation: historical and operational perspectives. Weather Forecast 20:351–366. doi:10.1175/WAF858.1

Bluestein HB (1992) Synoptic-dynamic meteorology in midlatitudes. Oxford University Press, Oxford

Changnon SA Jr (1968) The La Porte weather anomaly—fact or fiction? Bull Am Meteorol Soc 49:4–11

Chen F, Kusaka H, Bornstein R et al (2011) The integrated WRF/urban modelling system: development, evaluation, and applications to urban environmental problems. Int J Climatol 31:273–288. doi:10.1002/joc.2158

Childs PP, Raman S (2005) Observations and numerical simulations of urban heat island and sea breeze circulations over New York City. Pure appl Geophys 162:1955–1980. doi:10.1007/s00024-005-2700-0

Cleugh H, Grimmond CSB (2011) Chapter 3—urban climates and global climate change, 2nd edition. The future of the world's climate, pp 47–76. doi:10.1016/B978-0-12-386917-3.00003-8

Comarazamy DE, González JE, Luvall JC et al (2010) A land-atmospheric interaction study in the coastal tropical city of San Juan, Puerto Rico. Earth Interact 14:1–24. doi:10.1175/2010EI309.1

Dee DP, Uppala SM, Simmons AJ et al (2011) The ERA-interim reanalysis: configuration and performance of the data assimilation system. QJR Meteorol Soc 137:553–597. doi:10.1002/qj.828

Di Luca A, de Elía R, Laprise R (2015) Challenges in the quest for added value of regional climate dynamical downscaling. Curr Clim Change Rep 1(1):10–21. doi:10.1007/s40641-015-0003-9

Ebert EE, Janowiak JE, Kidd C (2007) Comparison of near-real-time precipitation estimates from satellite observations and numerical models. Bull Am Meteorol Soc 88:47–64. doi:10.1175/BAMS-88-1-47

Evans JP, Bormann K, Katzfey J, Dean S, Arritt RW (2015) Regional climate model projections of the South Pacific Convergence Zone. Clim Dyn (under review)

AQ3

Ganeshan M, Murtugudde R, Imhoff ML (2013) A multi-city analysis of the UHI-influence on warm season rainfall. Urban Clim.

doi:10.1016/j.uclim.2013.09.004

Gianotti RL, Zhang D, Eltahir EAB (2012) Assessment of the regional climate model version 3 over the Maritime Continent using different cumulus parameterization and land surface schemes. J Clim 25:638–656. doi:10.1175/JCLI-D-11-00025.1

Han J-Y, Baik J-J, Lee H (2014) Urban impacts on precipitation. Asia Pacific J Atmos Sci 50:17–30. doi:10.1007/s13143-014-0016-7

Haylock M, McBride J (2001) Spatial coherence and predictability of Indonesian wet season rainfall. J Clim 14:3882–3887

Hirpa FA, Gebremichael M, Hopson T (2010) Evaluation of high-resolution satellite precipitation products over very complex terrain in Ethiopia. J Appl Meteorol Climatol 49:1044–1051. doi:10.1175/2009JAMC2298.1

Holloway CE, Woolnough SJ, Lister GMS (2012) Precipitation distributions for explicit versus parametrized convection in a large-domain high-resolution tropical case study. QJR Meteorol Soc 138:1692–1708. doi:10.1002/qj.1903

Hong S-Y, Noh Y, Dudhia J (2006) A new vertical diffusion package with explicit treatment of entrainment processes. Mon Weather Rev 134:2318–2341. doi:10.1175/MWR3199.1

Huffman GJ, Bolvin DT, Nelkin EJ et al (2007) The TRMM multisatellite precipitation analysis (TMPA): quasi-global, multiyear, combined-sensor precipitation estimates at fine scales. J Hydrometeorol 8:38–55. doi:10.1175/JHM560.1

Janowiak JE, Kousky VE, Joyce RJ (2005) Diurnal cycle of precipitation determined from the CMORPH high spatial and temporal resolution global precipitation analyses. J Geophys Res 110:D23105–D23118. doi:10.1029/2005JD006156

Jauregui E, Romales E (1996) Urban effects on convective precipitation in Mexico city. Atmos Environ 30:3383–3389. doi:10.1016/1352-

2310(96)00041-6

Jourdain NC, Marchesiello P, Menkes CE et al (2011) Mesoscale simulation of tropical cyclones in the South Pacific: climatology and interannual variability. J Clim 24:3–25. doi:10.1175/2010JCLI3559.1

Joyce RJ, Janowiak JE, Arkin PA (2004) CMORPH: a method that produces global precipitation estimates from passive microwave and infrared data at high spatial and temporal resolution. J Hydrometeorol 5:487–503. doi:10.1175/1525-7541(2004)005<0487:CAMTPG>2.0.CO;2

Jullien S (2013) Ocean response and feedback to tropical cyclones in the South Pacific: processes and climatology, pp 1–229

Kidd C, Ferraro R, Levizzani V (2010) The fourth international precipitation working group workshop. Bull Am Meteorol Soc 91:1095–1099. doi:10.1175/2009BAMS2871.1

Kusaka H, Kimura F (2004) Coupling a single-layer urban canopy model with a simple atmospheric model: impact on urban heat island simulation for an idealized case. J Meteorol Soc Jpn 82:67–80

Kusaka H, Kondo H, Kikegawa Y, Kimura F (2001) A simple single-layer urban canopy model for atmospheric models: comparison with multi-layer and slab models. Bound-Layer Meteorol 101:329–358

Kusaka H, Nawata K, Suzuki-Parker A et al (2014) Mechanism of precipitation increase with urbanization in Tokyo as revealed by ensemble climate simulations. J Appl Meteorol Climatol 53:824–839. doi:10.1175/JAMC-D-13-065.1

Kwan MS, Tangang FT, Juneng L (2013) Present-day regional climate simulation over Malaysia and western Maritime Continent region using PRECIS forced with ERA40 reanalysis. Theor Appl Climatol 115:1–14. doi:10.1007/s00704-013-0873-5

Love BS, Matthews AJ, Lister GMS (2011) The diurnal cycle of precipitation over the Maritime Continent in a high-resolution

atmospheric model. QJR Meteorol Soc 137:934–947. doi:10.1002/qj.809

Mesinger F (2008) An essay on the eta cumulus convection (BMJ) scheme, pp 1–7

Mishra V, Ganguly AR, Nijssen B, Lettenmaier DP (2015) Changes in observed climate extremes in global urban areas. Environ Res Lett 10:1–10. doi:10.1088/1748-9326/10/2/024005

Neale R, Slingo J (2003) The Maritime Continent and its role in the global climate: a GCM study. J Clim 16:834–848. doi:10.1175/1520-0442(2003)016<0834:TMCAIR>2.0.CO;2

Oke T, Kłysik K, Bernhofer C (2006) Editorial: progress in urban climate. Theor Appl Climatol 84:1–2. doi:10.1007/s00704-005-0172-x

Prein AF, Langhans W, Fosser G et al (2015) A review on regional convection-permitting climate modeling: demonstrations, prospects, and challenges. Rev Geophys. doi:10.1002/(ISSN)1944-9208

Qian J-H, Robertson AW, Moron V (2010) Interactions among ENSO, the monsoon, and diurnal cycle in rainfall variability over Java, Indonesia. J Atmos Sci 67:3509–3524. doi:10.1175/2010JAS3348.1

Schmid PE, Niyogi D (2013) Impact of city size on precipitation-modifying potential. Geophys Res Lett 40:5263–5267. doi:10.1002/grl.50656

Shepherd JM (2005) A review of current investigations of urban-induced rainfall and recommendations for the future. Earth Interact 9:1–27

Shepherd JM, Burian SJ (2003) Detection of urban-induced rainfall anomalies in a Major Coastal City. Earth Interact 7:1–17

Skamarock WC, Klemp JB, Dudhia J et al (2009) A description of the advanced research WRF version 3. NCAR/TN-475 + STR NCAR technical note 125

Tan M, Ibrahim A, Duan Z et al (2015) Evaluation of six high-resolution satellite and ground-based precipitation products over Malaysia. Remote Sens 7:1504–1528. doi:10.3390/rs70201504

Teo C-K, Koh T-Y, Chun-Fung Lo J, Chandra Bhatt B (2011) Principal component analysis of observed and modeled diurnal rainfall in the Maritime Continent. J Clim 24:4662–4675. doi:10.1175/2011JCLI4047.1

Turk FJ, Xian P (2013) An assessment of satellite-based high resolution precipitation datasets for atmospheric composition studies in the Maritime Continent. Atmos Res 122:579–598. doi:10.1016/j.atmosres.2012.02.017

Ulate M, Dudhia J, Zhang C (2014) Sensitivity of the water cycle over the Indian Ocean and Maritime Continent to parameterized physics in a regional model. J Adv Model Earth Syst 6:1095–1120. doi:10.1002/2014MS000313

Vernimmen RRE, Hooijer A, Mamenun et al (2012) Evaluation and bias correction of satellite rainfall data for drought monitoring in Indonesia. Hydrol Earth Syst Sci 16:133–146. doi:10.5194/hess-16-133-2012

Wang Y, Zhou L, Hamilton K (2007) Effect of convective entrainment/detrainment on the simulation of the tropical precipitation diurnal cycle*. Mon Weather Rev 135:567–585. doi:10.1175/MWR3308.1

Wang Y, Long CN, Leung LR et al (2009) Evaluating regional cloud-permitting simulations of the WRF model for the tropical warm pool international cloud experiment (TWP-ICE), Darwin, 2006. J Geophys Res 114:D21203–D21221. doi:10.1029/2009JD012729

Wang X, Liao J, Zhang J et al (2014) A numeric study of regional climate change induced by urban expansion in the Pearl River Delta, China. J Appl Meteorol Climatol 53:346–362. doi:10.1175/JAMC-D-13-054.1

Yang GY, Slingo J (2001) The diurnal cycle in the tropics. Mon

Weather Rev 129:784–801. doi:10.1175/1520-0493(2001)129<0784:TDCITT>2.0.CO;2